The Visible Man Dataset in Medical Education: Electrophysiology of the Human Heart

C. D. Werner, F. B. Sachse, C. Baltes, O. Dössel

cw@ibt.etec.uni-karlsruhe.de

Institut für Biomedizinische Technik, Universität Karlsruhe, D 76128 Karlsruhe

http://www-ibt.etec.uni-karlsruhe.de

Abstract This work deals with the creation of a multimedia application for the medical education of the electrophysiology of the human heart. Different temporal and spatial distributions of physical fields are calculated by simulating the electrical excitation propagation based on an anatomical model of the Visible Man heart. The simulation is performed numerically by a cellular automaton for sinus rhythm as well as for pathological cases. In addition, the source current distribution is calculated and the body surface potential distribution is determined by means of a finite difference solver. These temporal and spatial physical field distributions are visualized using advanced methods of computer graphics. The visualizations consist of animations and interactively transformable 3D models. These animations and models are summarized on a HTML/VRML/Java based multimedia application for educational purposes.

Keywords Electrical Excitation Propagation, Cellular Automaton, Electromagnetical Fields, Digital Image Processing, Anatomical Models, MEETMan, Visualization, Medical Education

Contents

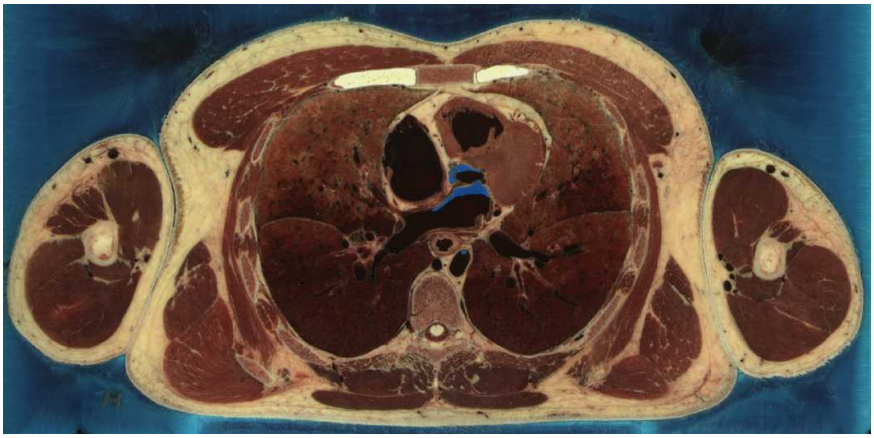

Figure 1: Cryosection of the Visible Man dataset: The layer displays a cross section through the Visible Man heart and the surrounding tissue.

1 Introduction

The mechanical contraction of the heart is coupled with the electrical excitation propagation of the myocardium. The electrical field distributions resulting from this excitation propagation usually vary depending on the time and the position in the three-dimensional space. Therefore it is difficult to depict the physical field distributions by means of conventional media. E.g. books are limited to the visualization of static two-dimensional figures.

This work deals with the creation of a multi media application for the medical education of the electrophysiology of the human heart. The visualized electrical fields are based on simulations of the propagation of electrical excitation within the human heart. The distributions of transmembrane potential, source current density, and electrical potential were calculated and visualized for sinus rhythm as well as for different pathologies. The visualizations consist of animations and 3D models providing information about the spatiotemporal field distribution.

2 Modeling the Human Anatomy

The electrical excitation propagation in the human heart depends on the anatomy of the heart, e.g. the different types of tissue and the spatial varying muscle fiber orientation is one parameter affecting the excitation propagation [1][2]. For a realistic simulation it is therefore necessary to represent the cardiac anatomy as accurate as possible.

In this work, the Visible Man dataset [3] of the National Library of Medicine, Bethesda, Maryland (USA) is used to derive a detailed anatomical model of the human body. Therefore different techniques of digital image processing [4] are applied to the cryosections (see figure 1) and CT scans of the Visible Man dataset. Initially, these images are preprocessed correcting alignment deficiencies by means of 2D correlation techniques [5]. Unusable or missing images of the dataset are interpolated applying an image morphing method based on radial basis transformations [5] (see figure 2). In a final preprocessing step the images are adjoined forming a multi-modal 3D dataset. To distinguish the different types of tissue in this 3D dataset different methods of 3D digital image processing are applied to segment and classify the dataset. Besides different filters, using 3D region growing (see figure 3) supported by interactively deformable surface meshes allowed the distinction of about 40 types of tissue. In figure 4, two three dimensional views of the classified datasets are displayed.

In order to include the anisotropic properties of the skeletal and cardiac muscles, the orientation of the muscle bundles are determined by means of a texture analysis [6]. Therefore, for a set of user

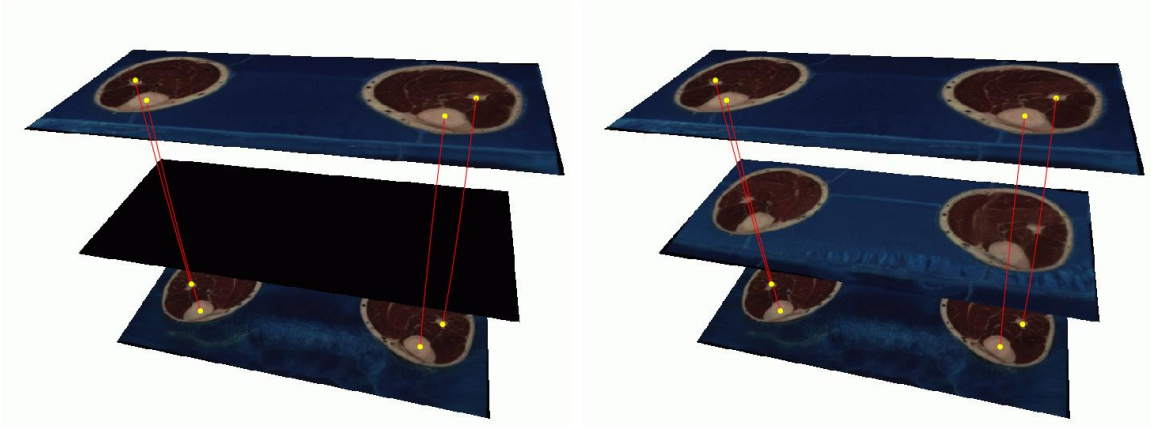

(a) (b)

Figure 2: The figure shows the Visible Man cryosections below the knees before (a) and after (b) the interpolation with the radial basis transformations. The yellow dots in the upper and lower layers mark the locations of corresponding anchor points which determine the transformation.

defined locations in the heart, the principle components are calculated and interactively corrected by means of a 3D editor. Thus, the muscle fiber orientation of each volume element of this set is represented by the solid angle of the first principle component. To obtain the fiber orientation of the

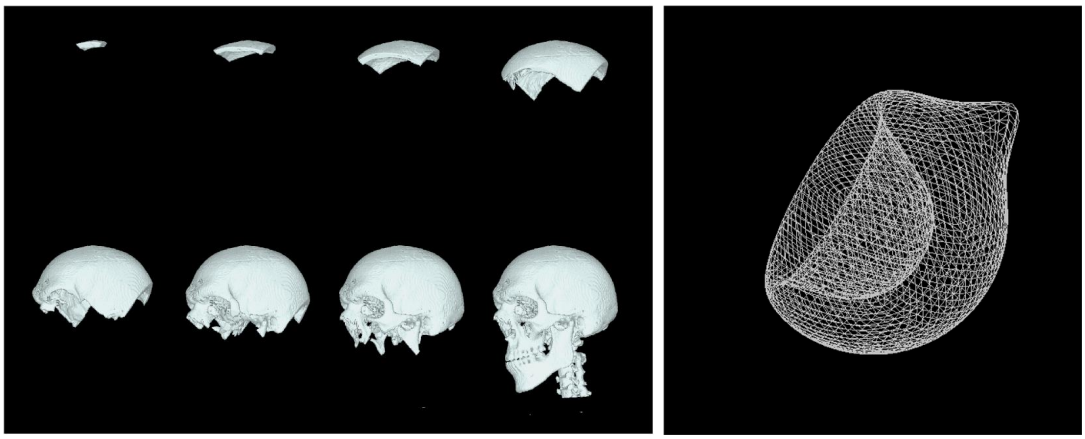

(a) (b)

Figure 3: Figure (a) shows an exemplary segmentation of the skull using a 3D region grower. The segmentation starts at a seed point at the top of the skull. Outgoing from this seed point the color values of the neighboring volume elements are evaluated. Those neighboring volume elements that meet user defined requirements to the color value are taken as seed point in the next following evaluation step. This iterative process finishes if no more suitable neighbor volume elements are found. To avoid false classifications the region growing process is supported by interactively deformable surface meshes. Thus, adjacent tissue types of similar color can be separated. The right figure shows one deformed surface mesh.

remaining volume elements, an iterative interpolation algorithm is applied to the cardiac and skeletal muscle domains. The cardiac fiber orientation is displayed in figure 5.

The temporal and spatial propagation of the electrical excitation is strongly affected by the specialized cardiac conduction system. It consists of specialized muscle fibers building an arboreal structure connecting the atrio-ventricular node with the Purkinje fiber endings through the bundle of His and the left and right bundle branches. Due to the small size of these specialized fibers and due to the similarity of its colors to the colors of the adjacent tissue it is hardly possible to segment the conduction system based on the Visible Man data. Therefore, in this work, it is built semi-automatically. It is represented by a tree connecting nodes by edges. For the majority of the nodes the location is determined automatically. Only few nodes are determined by user interaction, e.g. the atrio-ventricular node and few nodes of the left and right bundle branches. The connection between the nodes is calculated automatically applying a variant of Prim's algorithm [7] to find the shortest subspanning tree within all nodes and edges. The specialized cardiac conduction system is shown in figure 6.

3 Modeling the Cardiac Electrophysiology

The simulation of the electrophysiologic cardiac behavior is performed by means of a cellular automaton, which calculates the temporal and spatial distribution of the transmembrane potential of the cardiac cells [8]. The excitation of one cardiac cell is propagated to its neighbor cells with regard to the electrophysiologic properties of the cells. These properties are derived from models of cellular electrophysiology as described in [9][10]. The properties are described by different parameters, e.g. the location, the type of tissue, the fiber orientation, the excitation velocity and the frequency of excitation. All parameters affect the shape of the transmembrane potential course of each cell and therefore the calculation result of the cellular automaton. The number of parameters considered by the cellular automaton determines the number of states of the cellular automaton. In figure 7 a partial state diagram of the cellular automaton is displayed.

In a further step the source current density is calculated outgoing from the simulated transmembrane potential distribution using a bidomain model [11] which averages the extra cellular and intra-

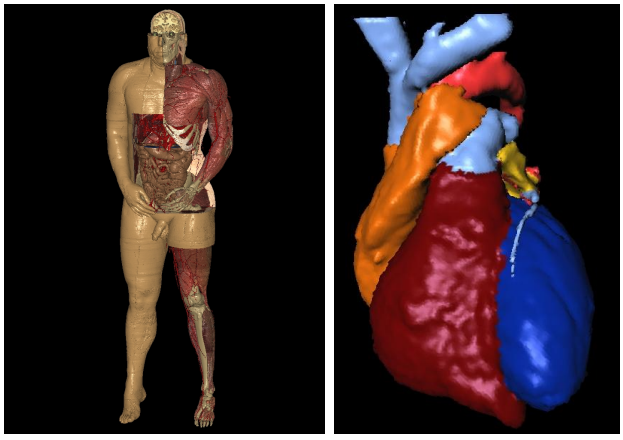

(a) (b)

Figure 4: The left image shows the segmented and classified body model derived from the Visible Man. The right image displays the surface of the Visible Man heart. Both are part of the MEET-Man project, which deals with the creation of **M**odels for the simulation of **E**lectromagnetic, **E**lastomechanic and **T**hermic behavior of **Man**.

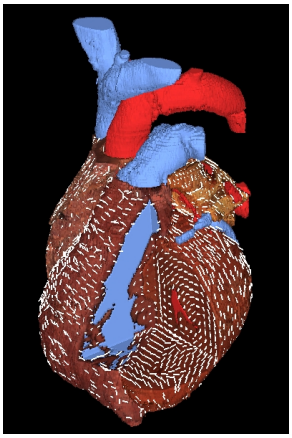

Figure 5: The white lines depict the fiber orientation displayed on the surface of the Visible Man heart. In the area of the interventricular septum the heart is cut to provide a view onto the endocardium.

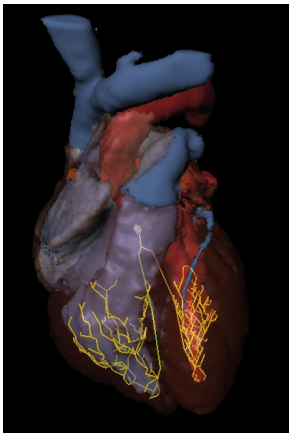

Figure 6: The specialized cardiac conduction system is shown in the anatomical context. Therefore, the epicardium is displayed semi-transparently. At the left and right ventricular endocardium, the blood is displayed in red and blue color, respectively. In addition, the location of the sino-atrial node is displayed in the right atrium in orange color.

cellular space into two domains of the same location separated at each point by the cell membrane. The electrical sources I_m are calculated from the transmembrane potential Φ_m with regard to the effective intracellular conductivity tensor $\vec{\sigma_i}$ as follows [11]:

$$I_m = \nabla \vec{J^i} = -\nabla \left(\vec{\sigma_i} \nabla \Phi_m \right)$$

where $\vec{J^i}$ is the impressed current density.

Finally, this source current distribution is used to calculate the electrical potential distribution in the entire body. Therefore the generalized Poisson equation

$$\nabla \left(\vec{\sigma} \nabla V \right) = I_m$$

where V is the extracellular potential and $\vec{\sigma}$ is the conductivity tensor, is solved by means of a finite difference multi-grid solver regarding the heterogeneous anisotropic tissue distribution [12]. In addi-

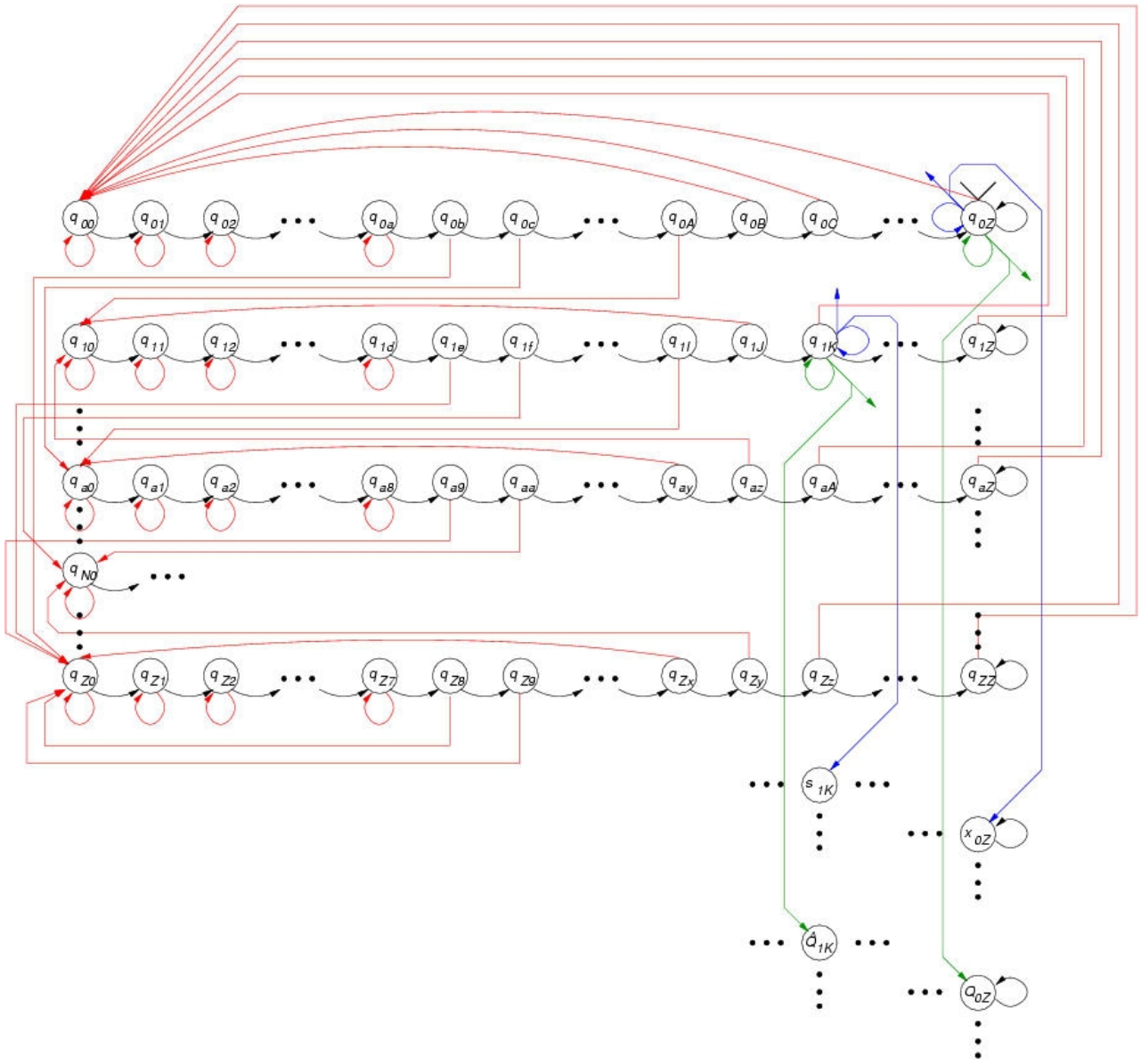

Figure 7: Partial state diagram of the finite automaton working on each cell of the cellular automaton: The alphabet of the automaton contains four elements displayed as differently colored arcs. Black arcs depict the increment of time while running the cellular automaton, red arcs a stimulus generated due to excitation propagation, autorhythmicity or external interaction. Green arcs describe the alternation of the tissue class and therefore the change of the electrophysiological tissue characteristics. Any change of fiber orientation is represented by the blue arcs.

tion, the standard electrocardiograms (ECG) are calculated by evaluating the potential distribution on the body surface.

Changing the anatomical or electrophysiologic properties of the tissue facilitates the simulation of pathologies. E.g. by cutting the specialized cardiac conduction system at the right bundle branch it is possible to simulate a right bundle branch block. By changing the shape of the transmembrane potential course and therefore the excitation velocity and refractory periods it is possible to simulate flutter and fibrilation as well as an infarction. Adding pathways from the atrial to the ventricular

myocardium enables the simulation of the Wolff-Parkinson-White syndrome.

4 Results

Several simulations are performed applying the cellular automaton to the anatomical model of the Visible Man heart including the sinus rhythm as well as simulations of a right bundle branch block, a Wolff-Parkinson-White syndrome and an infarction. The simulation results are visualized applying different methods of computer graphics. These methods include surface based opaque visualizations as well as semi-transparent volume based visualizations of the field distributions. Animations of electrical fields related to the electrical excitation propagation in the heart are created as well as interactively manipulable 3D scenes of the cardiac anatomy. Along with textual descriptions of the cardiac anatomy and electrophysiology, images, the animations and 3D scenes are summarized in a HTML/VRML/Java based application.

Some exemplary animations are listed here: The first animation shows the electrical excitation propagation of a sinus rhythm. The transmembrane potential distribution is shown in figure 8. In figure 9 the source current distribution of an transmural infarction in the left ventricular free wall is visualized with a semi-transparent heart surface. Figure 10 shows the body surface potential map of a right bundle branch block. Figure 11 shows an electrocardiogram (ECG) of the right bundle branch block in comparison to the sinus rhythm ECG.

Future work will focus on cardiac motion and the simulation of the elasto-mechanical contraction of the heart. The simulation of surgical interventions may be included in future work as well.

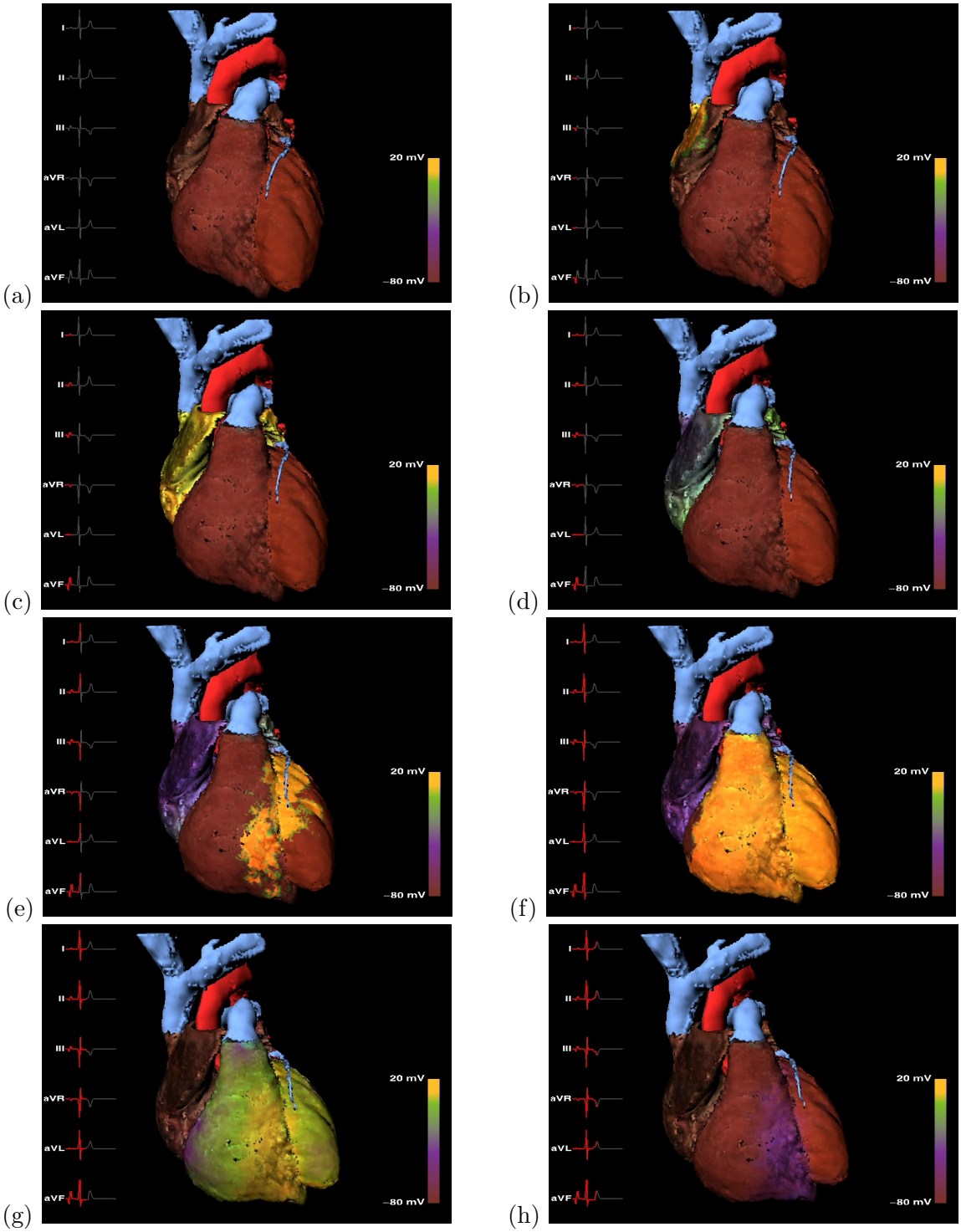

Figure 8: Simulation of a sinus rhythm: The transmembrane potential is displayed color-coded on the surface of the heart. The excitation starts in the sino-atrial node located in the right atrium near the superior vena cava. The excitation propagates over the atria. Reaching the atrio-ventricular node the excitation propagates through the specialized cardiac conduction system towards the Purkinje fiber endings. Once the Purkinje fiber endings are reached, the excitation is spread all over the ventricles.

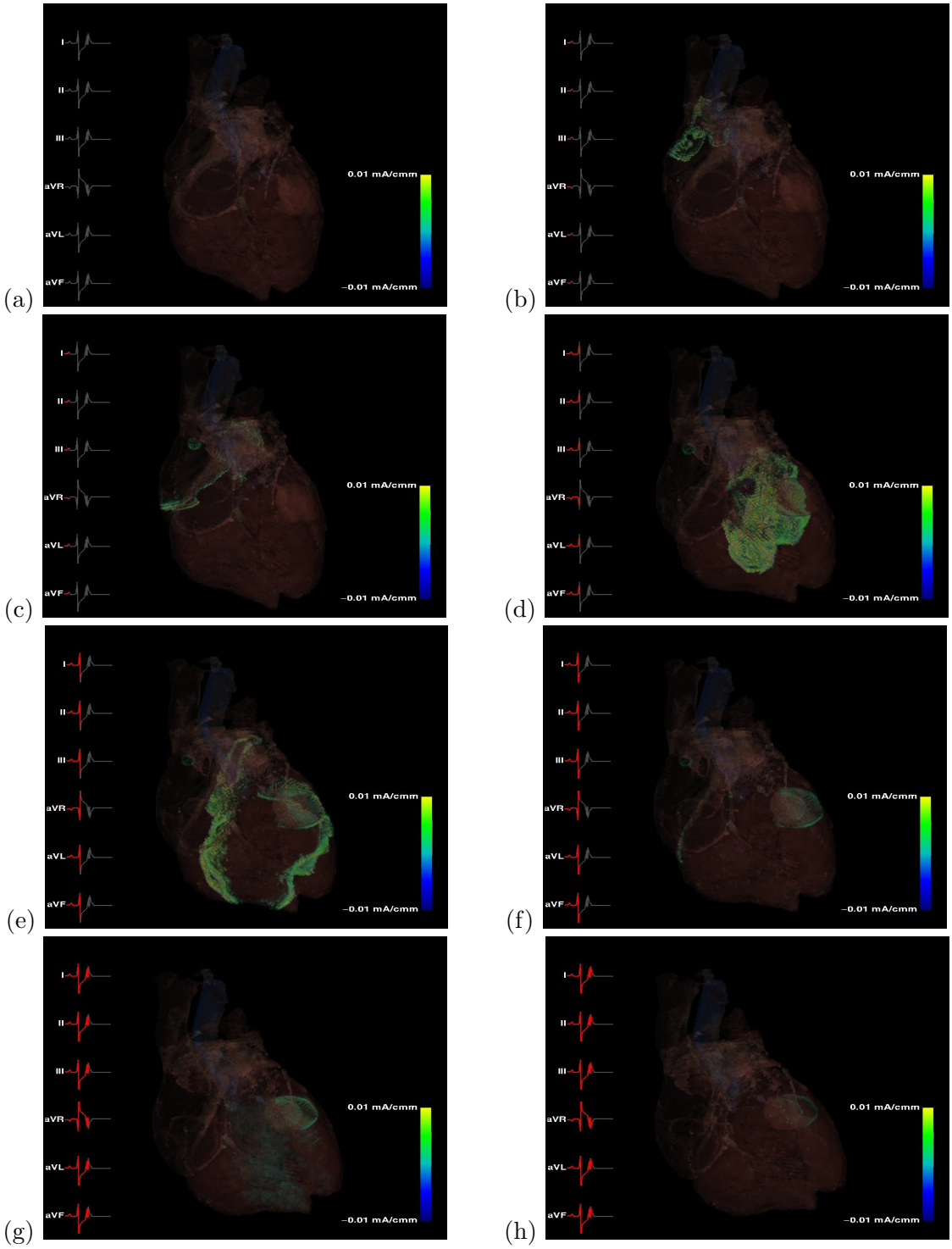

Figure 9: Simulation of a transmural infarction: The infarction is located in the left ventricular free wall. The source current distribution is displayed in this image sequence. In the area of the infarction the excitation properties are changed. Thus, the repolarization is delayed and the ST interval in the ECG is lowered.

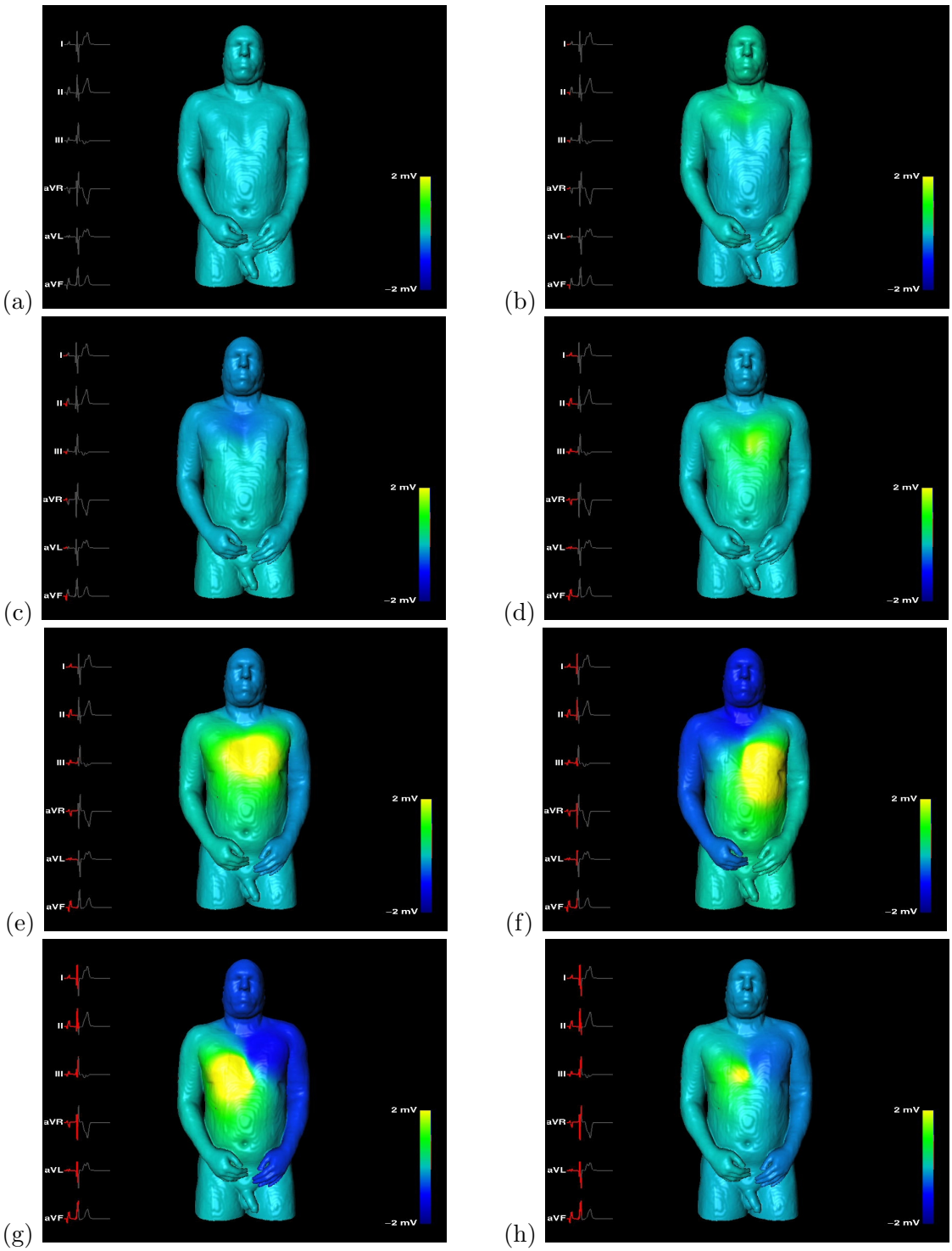

Figure 10: Simulation of a right bundle branch block: The body surface potential map is displayed color-coded.

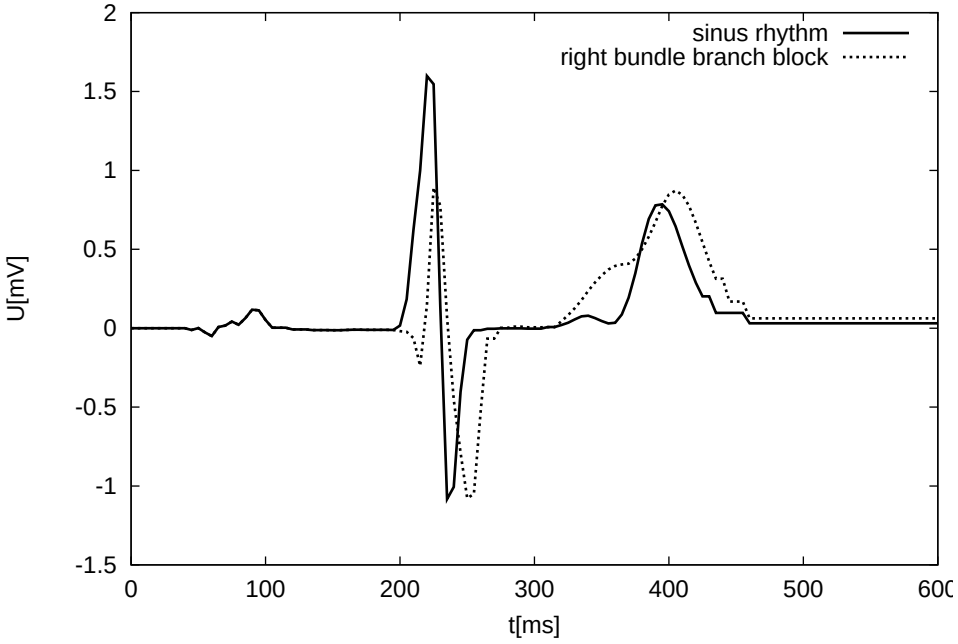

Figure 11: The Einthoven I lead of the simulation of a right bundle branch block is depicted in comparison to the sinus rhythm electrocardiogram.

References

[1] C. D. Werner, F. B. Sachse, and O. Dössel, "Vergleichende Betrachtung von isotropen und anisotropen Modellen der Erregungsausbreitung im Herzen," in *Biomedizinische Technik*, vol. 43, pp. 69–70, 1998.

[2] F. B. Sachse, C. D. Werner, K. Meyer-Waarden, and O. Dössel, "Comparison of solutions to the forward problem in electrophysiology with homogeneous, heterogeneous and anisotropic impedance models," in *Biomedizinische Technik*, vol. 42-1, pp. 277–280, 1997.

[3] M. J. Ackerman, "Viewpoint: The Visible Human Project," *Journal Biocommunication*, vol. 18, no. 2, p. 14, 1991.

[4] R. C. Gonzalez and R. E. Woods, *Digital Image Processing*. Reading, Massachusetts; Menlo Park, California: Addison-Wesley, 1992.

[5] F. B. Sachse, C. D. Werner, M. Müller, and K. Meyer-Waarden, "Preprocessing of the Visible Man dataset for the generation of macroscopic anatomical models," in *Proc. First Users Conference of the National Library of Medicine's Visible Human Project*, pp. 123–124, 1996.

[6] F. B. Sachse, M. Wolf, C. D. Werner, and K. Meyer-Waarden, "Extension of anatomical models of the human body: Three dimensional interpolation of muscle fiber orientation based on restrictions," *Journal of Computing and Information Technology*, vol. 6, no. 1, pp. 95–101, 1998.

[7] T. H. Cormen, C. E. Leiserson, and R. L. Rivest, *Introduction to Algorithms*. Cambridge/Massachusetts: The MIT Press, 1990.

[8] C. D. Werner, F. B. Sachse, and O. Dössel, "Electrical excitation propagation in the human heart," in *CardioModel 2000, Computer Models of the Heart: Theory and Clinical Application*, vol. 2-2, International Journal of Bioelectromagnetism, September 2000. ISSN 1456-7865.

[9] Y. E. Earm and D. Noble, "A model of single atrial cell: Relation between calcium current and calcium release," *Proc. R. Soc. Lond.*, vol. 240, pp. 83–96, 1990.

[10] D. Noble, A. Varghese, P. Kohl, and P. Noble, "Improved guinea-pig ventricular cell model incorporating a diadic space, I_{Kr} and I_{Ks}, and length- and tension-dependend processes," *Canadian Journal of Cardiology*, vol. 14, pp. 123–134, Jan. 1998.

[11] D. B. Geselowitz, "On the theory of the electrocardiogram," *Proceedings of the IEEE*, vol. 77, pp. 857–876, June 1989.

[12] F. B. Sachse, C. D. Werner, K. Meyer-Waarden, and O. Dössel, "Applications of the visible man dataset in electrocardiology: Calculation and visualization of body surface potential maps of a complete heart cycle," in *Proc. Second Users Conference of the National Library of Medicine's Visible Human Project*, pp. 47–48, 1998.